WIND ACCELERATION PROCESSES

RAPPORTEUR PAPER IV

Peter Wurz* and Alan H. Gabriel**

*Weltraumforschung und Planetologie, Physikalisches Institut, Universität Bern
Sidlerstrasse 5, CH-3012 Bern, Switzerland
Tel.: (+41 31) 631 44 26 / FAX.: Tel.: (+41 31) 631 44 05, e-mail: peter.wurz@soho.unibe.ch

**Institut d'Astrophysique Spatiale (IAS), Unité Mixte Centre National de la Recherche Scientifique/Université Paris XI, Bâtiment 121, F-91405 Orsay, France
Tel.: (+31 1) 69 85 85 10 / FAX.: Tel.: (+31 1) 69 85 86 75, e-mail: gabriel@iaslab.ias.fr

ABSTRACT

The topic of this working group was divided in four subtopics with the titles: i) Coronal hole structures, ii) Polar plumes: Is there a two-component plasma in the holes? iii) Fast wind acceleration region, and iv) Origin of slow solar wind. The first two points were discussed virtually together during the working group sessions. In this review we reversed the order of these points, since the question of the two-component plasma in coronal holes has to be addressed to proceed with the structure of the coronal holes.

1. POLAR PLUMES: IS THERE A TWO-COMPONENT PLASMA IN CORONAL HOLES

This question was addressed extensively by the working group and there is growing experimental evidence for a two-component plasma in coronal holes. The interpretation favored by the members of the working group is that there are polar plumes (the bright features in the polar corona) and there are the inter-plume lanes (the less bright plasma between the plumes). Polar plumes are radial at the pole and non-radial at the border of the coronal hole. A typical image of polar plumes is shown in Figure 1, which was recorded with SUMER/SOHO. The life time of a plume is typically one day. Depending on observation wavelength (i.e., a particular ion line) or white-light observations, some of these polar plumes can be observed out to distances of six and more solar radii.

During the working group session distinct plasma parameters were reported for these two plasma components which we will summarize here. From lines ratios of Si VIII lines (1445 Å, 1440 Å) the electron density in plumes was derived, which starts to depart from the surrounding medium around 1.2 $R_\odot$ and is up to a factor of three larger in the plumes than in the inter-plume lanes

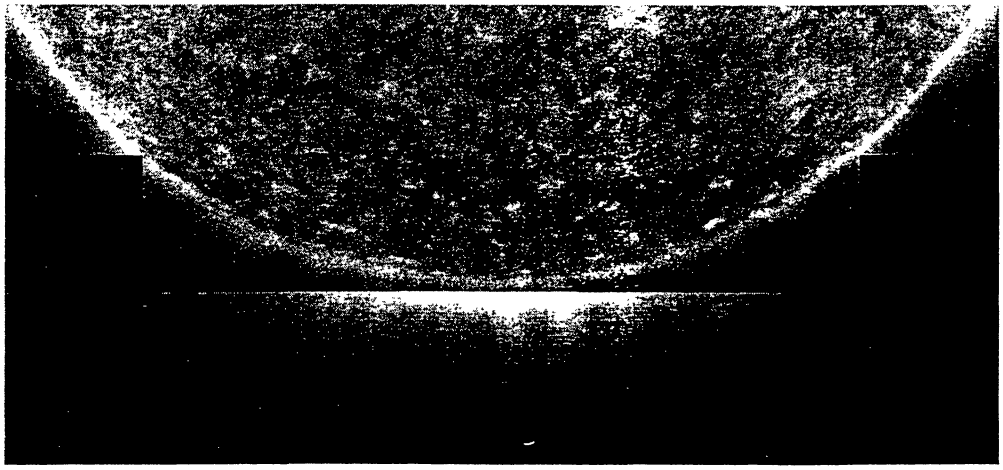

***Figure 1**: South polar coronal hole with bright points and plumes seen in the Ne VIII (λ770 Å) emission line, which is formed at about 630 000 K. The image was recorded by SUMER/SOHO on February 2/3, 1996 (from Wilhelm et al. [1]).*

Proceedings 8th SOHO Workshop 'Plasma Dynamics and Diagnostics in the Solar Transition Region and Corona', Paris, France, 22-25 June 1999, (ESA SP-446, October 1999)

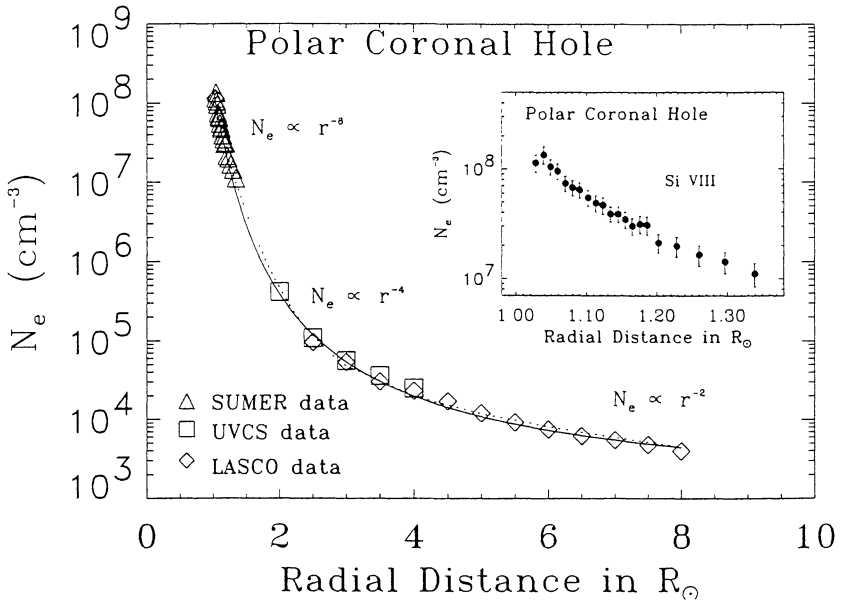

***Figure 2**: Profile of the electron density above the polar coronal hole (from Doyle et al. [10]). The circles represent the data from SUMER, the diamonds data from LASCO, and the triangles data from UVCS. The solid line represents a theoretical model with $T_{eff} = 1.2 \cdot 10^6$ K and the dashed line represents the polynominal fit given in eq. 1.*

[2, 3]. Also, the electron temperature is lower in the plumes. Both observations are discussed in detail below. The ion temperature is higher in the inter-plume lanes than in the plumes. This is seen in the line widths of hydrogen and of oxygen ions and increases with height (see review by Antonucci [4]) and is more pronounced for the oxygen ions. Also the outflow velocities are different. From UVCS/ SOHO observations at 1.7 $R_\odot$ it was found that the outflow velocity for O^{5+} in the plume is $\leq 45(+25)$ km/s, and for the inter-plume plasma it is $115(-15) \leq v \leq 175(+40)$ km/s. Similar observations were reported using SUMER/SOHO measurements of the Doppler-shifted He I (584 Å) and Ne VIII (770 Å) lines [5]. Closer to the solar surface strong outflow was predominately correlated with the low intensity regions of the coronal hole, i.e., the inter-plume areas. The average Doppler shift amounts to 3 km/s both for He I and for Ne VIII. However, if considering only regions of strong outflow, the typical outflow speed is 10 km/s.

The considerably larger outflow velocities in the inter-plume lanes seem to suggest that the solar wind from polar coronal holes might originate mainly from these locations. This was concluded from the recent Doppler shift measurements of He I and Ne VIII lines by Wilhelm et al. [5] and from the UVCS measurements by Antonucci [4]. However, this simple picture is problematic because it is difficult to see how the, presumably static, plumes are held in place. If there is no upward flow in these plumes they should collapse. Wave heating is a possible mechanism to support the plume. Recently, density variations in coronal holes on a time scale of 9.3±0.4 minutes were reported [6, 7]. Also structures within the plumes propagating outwards at velocities of ≈ 75–150 km/s and recurring quasi-periodically on time scales of approximately 10 minutes were found recently [8]. These fluctuations have been interpreted as slow magneto-hydrodynamic waves, which are confined to the plumes and steepen while rising up, and may contribute to the local heating [9]. Possibly these waves also exist in the inter-plume plasma and have not been observed so far because of the low light emission from these areas.

2. CORONAL HOLE STRUCTURES

It is of fundamental importance to understand the structure of the coronal hole for the understanding of the solar wind acceleration. All solar wind modeling requires the knowledge of density and temperature at the base of the corona as a boundary condition. The radial profiles of the electron density and temperature are important observables any theoretical model has to reproduce. A large fraction of the discussions was spent on these questions and will be reviewed here. What is also important is the knowledge of the large-scale geometry of the coronal magnetic field. The white-light polarized brightness observations can provide both the density and the divergence of flow structures and flux tubes.

Electron densities can be either derived from line ratios (e.g., Si IX 350/342 Å) or from measurements of the polarization brightness using coronagraphs. Each method has its own strengths and problems. Figure 2 shows the electron density in a polar coronal hole from close to the limb out to 8 $R_\odot$ as was derived from SUMER, UVCS, and LASCO data [10]. At the coronal base they find an

electron density of $1 \cdot 10^8$ cm^{-3}. The authors gave a polynomial fit to the data

$$n_r = \frac{10^8}{r^8} + \frac{2.5 \cdot 10^8}{r^4} + \frac{2.9 \cdot 10^8}{r^2} \quad [cm^{-3}] \qquad \text{Eq. 1}$$

Similar electron density profiles and fits to the data have been reported recently by several groups [11-13] and are reproduced in Figure 3. Note that this compilation of reported electron density profiles is not a complete list, there are many more such reports in earlier work. The profiles derived from UVCS measurements show a rather high density at the coronal base ($3.8 \cdot 10^8$ cm^{-3}), but agree with Figure 2 and Eq. 1 from 1.8 $R_\odot$ outwards reasonably well [11]. The profiles derived from CDS and Mauna Loa white-light coronagraph data [12] show a density at the coronal base of $1.8 \cdot 10^8$ cm^{-3} and $2.4 \cdot 10^8$ cm^{-3} for the polar coronal hole (i.e., the inter-plume plasma) and the polar plume, respectively, and the electron density falls off faster with radial distance than reported in [10]. Electron densities and a polynomial fit were also derived from the Spartan White Light and Mauna Loa measurements [13], and are similar to the one presented in Figure 2. However, the authors find the density at the coronal base to be rather high ($3.7 \cdot 10^8$ cm^{-3}), and again the density falls off faster with radial distance than reported in [10]. Figure 3 shows that there is large the scatter between the different measurements.

This difference possibly arises from the theoretical interpretation of the data. Also, the densities will come out differently if plumes and inter-plume areas are not resolved, which is the case for work reported in [10, 11, 13]. Wilhelm et al. [3] reported electron density measurements were plumes and inter-plume plasma has been resolved, which show that the electron densities agree at the coronal base at value of $1 \cdot 10^8$ cm^{-3} (shown in Figure 4). However, the electron density falls-off much steeper in the inter-plume lanes than for the plumes with increasing height. At 1.3 $R_\odot$ the electron density is already about a factor four higher in the plumes than in the inter-plume lanes.

It is important to fix the electron density in the first scale height at the base of the corona, which form an essential boundary condition for the onset of the solar wind. The analyses cited above depend either on the line ratio analysis of spectral lines, or on polarised brightness measurements using coronagraphs. The first method is limited by the precision of the atomic physics employed and a full error analysis of this technique is rarely included. Coronagraphs suffer from the difficulty of stray light correction, which is always more severe close to the limb.

It might be thought that polarized brightness measurements carried out during total solar eclipses would avoid all of these problems and therefore give potentially more reliable data. Such observations give coronal electron densities at the base consistently lower than the values quoted above. For the polar coronal hole a base density of $1.8 \cdot 10^7$ cm^{-3} has been reported by Koutchmy [14], which has been reproduced at later eclipses. It is also found that the ratio of this base density, between quiet closed equatorial regions and polar holes lies typically between 7 and 15, with a mean value around 10. This is in striking contrast to the ratio of 2 or 3 found from line-ratio techniques. This discrepancy between the different base density determinations was highlighted in the Working Group. The LASCO teams undertook to look carefully at their latest calibrations and to try to refine their contribution to this problem. There is also some level of support from LASCO data for such

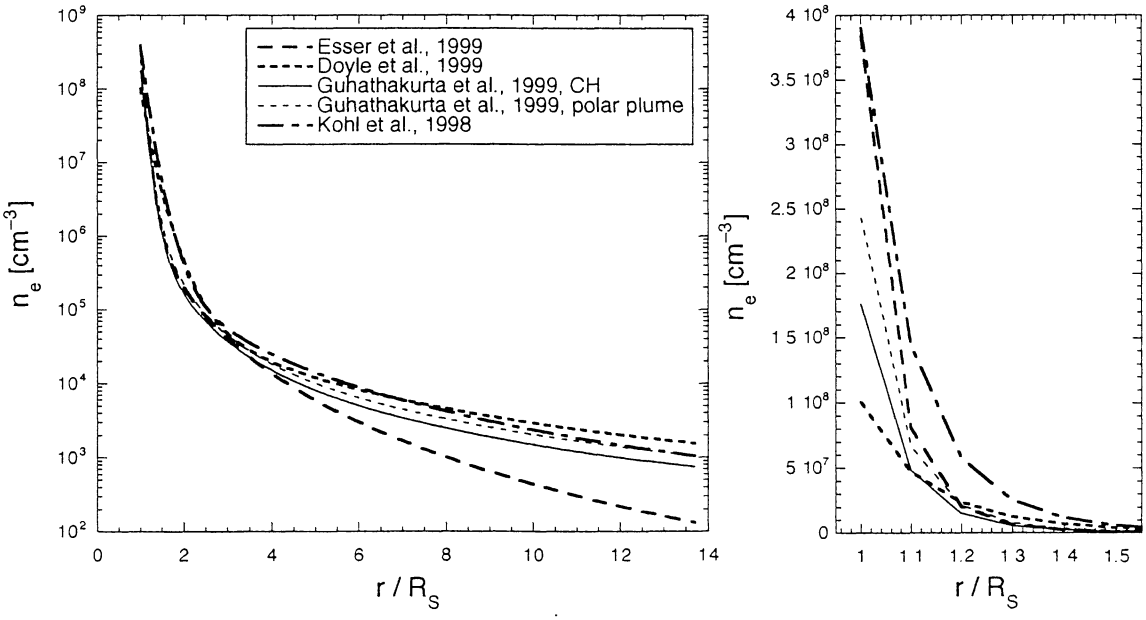

***Figure 3**: Compilation of the electron density profiles above the polar coronal hole as reported by several groups [10-13]. The right panel shows the same data close to the solar surface with a linear vertical scale.*

a low electron density at the base. Two-dimensional maps of electron densities for heights $> 2\ R_\odot$ from Thompson scattering will be shortly available from LASCO (A. Llebaria and co-workers and R. Howard and co-workers), both for the fast and slow wind regions. These measurements are eagerly awaited by the community, in particular, given high value and scatter in the reported results (see also Figure 3).

The electron temperature in the corona is derived from line ratios. In Figure 5 the electron temperature close to the Sun is shown [15]. The electron temperature in the polar coronal hole is different for the plume and the inter-plume plasma. The curve in the figure marked with coronal hole is representative for plume plasma, since the electron density is about a factor four higher in plumes above a certain height (see Figure 4). For the inter-plume plasma the electron density remains approximately constant at 800'000 K out to $1.6\ R_\odot$ (from [3] and K. Wilhelm, private communication).

A detailed study of the August 1996 equatorial coronal hole (also known as the Elephant's Trunk coronal hole) by Del Zanna and Bromage [16] showed that it has very similar physical parameters as polar coronal holes (that is, electron temperature, density, and element abundance). Also plumes were found in this equatorial coronal hole, with very similar physical properties as plumes in polar coronal holes. Also the *in situ* particle data show the enhancements of low-FIP elements typical for coronal hole plasma, however, the solar wind speed at 1 AU was significantly lower than has been observed for polar coronal holes [17].

2.1. Fast wind acceleration region

The fast solar wind is thought by many to be the basic mode of the solar wind. Its origin has been associated with coronal holes already since the mid 70's [18]. It is a stable flow with velocities > 700 km/s. The heavier elements (alpha particles and heavy ions) move even faster than the protons, with a typical excess velocity comparable to the Alfvén speed [19-22].

Observations

Many details of observations regarding the solar wind acceleration can be found in the review of Antonucci [4]. Thus, the observations are only summarized very briefly here. Particle outflow velocities were measured with UVCS/SOHO for hydrogen and oxygen ions by doppler diming of the hydrogen Lyman α line (1216 Å) and the ratio of dimmed emissions of O VI lines (1037 Å, 1032 Å) [11]. Fast acceleration of particles, on average 60 m/s^2 between 1.6 and 3 $R_\odot$, is observed for coronal holes for a time period near solar minimum. Within a few solar radii velocities of several hundred km/s are reached, with the heavy ions accelerated faster and to higher values than the protons [11]. However, the faster acceleration of heavy ions is still under debate [4].

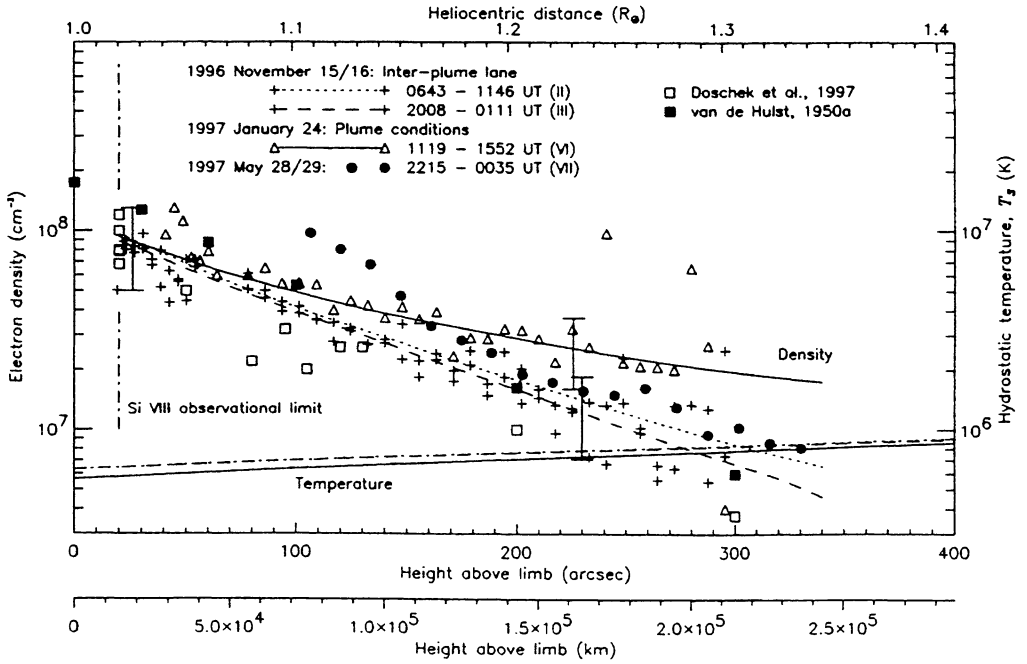

***Figure 4**: Electron densities derived from the Si VIII line ratios and a comparison with the data in the literature (from Wilhelm et al. [3]). The hydrostatic temperature, T_S, used for the fits of the line Si VIII (1445 Å) is plotted in the lower portion of the diagram, with the scale on the right-hand side. The error bars indicate a density variation resulting from a ±30% uncertainty in the line ratio determination. Note that there is a small (≤ 3%) seasonal variation between the angular and the spatial scales for different data sets.*

From radio scintillation measurements it has been concluded that the asymptotic interplanetary velocity is reached within 10 $R_\odot$ [23]. Also heating of the particles occurs rather close to the Sun. Within 2–3 solar radii effective temperatures of 4 MK and 300 MK for hydrogen and O^{5+} are observed. Thus, the ion temperatures scale with ion mass more than mass proportional [4, 11]). Such high ion temperatures in the solar corona have recently also been reported for Mg ions [13]. Thus, heavy ions are neither in thermal equilibrium with the protons nor with the electrons. Probably, the electrons and protons decouple near 1.2–1.3 $R_\odot$, and the heavy ions decouple from the protons roughly at 1.5 $R_\odot$. Using the hydrogen Lyman series the hydrogen temperature, and with some model assumptions also the proton temperature and density at the base of the corona (at $\approx 0.02\ R_\odot$) were determined to be 100'000–200'000 K and $(1–2)\cdot 10^8$ cm^{-3}, respectively [24]. Moreover, a strong anisotropy of the kinetic temperatures perpendicular and parallel to the magnetic field is observed for O^{5+} (O VI lines), with $T_\perp$ much higher than $T_\parallel$, by a factor of 10 and more [11].

Theory

Most of the modeling of solar wind acceleration has concentrated on fast solar wind so far, because of its simpler nature than the slow solar wind and because it can be treated with steady-state theory. A successful theoretical model for the solar wind acceleration has to reproduce the experimental observations, which are for the fast solar wind:

- The asymptotic speed is $v_\infty \approx 750 – 800$ km/s, from Ulysses measurements [25].
- The particle flux at 1 AU is $f \approx 2.4\cdot 10^8$ / (cm^2 s), from Ulysses measurements [25].
- The average proton and electron temperatures at 1 AU are $T_p \approx 200'000$ K and $T_e \approx 100'000$ K.
- The mean momentum flux is $f_m \approx 1.4\cdot 10^{18}$ amu/(m s^2).
- The helium abundance relative to hydrogen is 0.043±0.06, from measurements performed with Ulysses [26].
- Large temperature anisotropy of ions, $T_\perp > T_\parallel$.
- Minor ion species have a temperature, which is more than mass proportional to the protons, $T_i > (m_i/m_p)\ T_p$.
- Most of the acceleration of the solar wind is within the first $R_\odot$ [11], and the solar wind is fully developed already at 10 $R_\odot$ [23].
- The electron temperature is low, around 1 MK and below.
- The electron density at the base of the corona is low, in the range of $(2 – 10)\cdot 10^7$ cm^{-3}, see also the discussion above.

Since a theoretical model for the solar wind acceleration also has to include the solar atmosphere and the coronal heating, a few other observed properties have to be reproduced by the model [27], which are not listed here.

Adequate description of the problem of solar wind acceleration made it necessary to use multi-fluid models. Two-fluid models (electrons and protons) have been

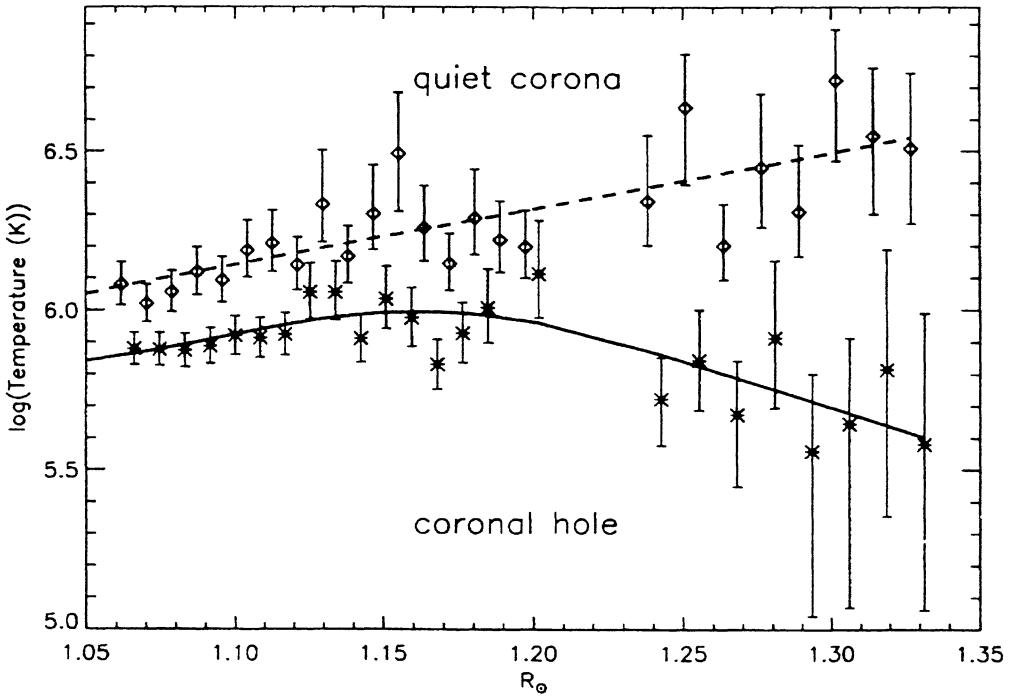

***Figure 5**: Temperature gradient measurement in the quiet corona (equatorial west limb) and the north polar coronal hole (from David et al. [15]). Observations were carried out on 21 May 1996, measured with the CDS and SUMER instruments on SOHO.*

used widely, but there are also some studies using three-fluid models (electrons, protons, and alpha particles) [28-30], and even four-fluid models [31, 32]. The four-fluid model by Hu et al. [32] also included O^{5+} ions to compare directly the derived properties with UVCS results.

It was recognized already several years ago that coronal heating and solar wind acceleration most likely have to be considered together, since the corona supplies the energy and momentum that sustains the solar wind. Note that at this workshop there was a separate working group dedicated to "Coronal heating and structure". An additional source of mechanical energy is necessary for the solar wind acceleration since heat conduction alone cannot produce the high proton temperatures that are observed and which are necessary to produce the measured mass flux. The current understanding is that heating by dissipation of Alfvén waves is the most promising candidate of this additional energy source for solar wind acceleration from coronal holes, although the details of the mechanism(s) are largely unknown. The UVCS results indicate that the heating in coronal holes acts mainly on the transverse degrees of freedom suggesting that the heating is occurring via the ion-cyclotron resonance. The waves heat the ions more than mass proportional and once the ions are hot enough they would be pushed out by their own pressure gradient.

The heating function in the energy equation, which provides the temperature maximum close to the solar surface and the fast acceleration of the wind, is one of the major pieces distinguishing the different theoretical models. Depending on the number of fluids in the model, separate heating functions for electrons, protons, alpha particles and perhaps even for the minor ion can be specified. In the simplest form an unspecified heat source is prescribed with its free parameters optimized to reproduce the observed temperature and acceleration profiles [27, 29]. The heating function has to have a characteristic dissipation length of less than one $R_\odot$ to obtain the fast wind acceleration. Also, the maximum expansion of the flow tubes is an important fitting parameter in the models to obtain fast acceleration.

In an extensive modeling effort, Tu and Marsch used the dissipation of high-frequency Alfvén waves (0.8 Hz to 800 Hz) via cyclotron damping to heat the corona and accelerate the solar wind [33]. The waves are assumed to be generated by the small-scale magnetic activity in the chromospheric network and the power spectra are based on observations performed at 0.3 AU of low frequency Alfvén waves, and are extrapolated to higher frequencies and to closer distances to the Sun using WKB theory. A spectral index of -1 was chosen. In other works the spectral index ranges from $-1 \leq \gamma \leq -2$. In order to reproduce the observed properties certain frequency ranges were given additional power. This model describes well the observed general properties of the solar corona and the high-speed solar wind emanating from coronal holes. However, the large anisotropy in $T_\perp$ and $T_\parallel$ is not reproduced by this model. A similar approach has been taken recently by Cranmer et al. [34], who can also reproduce the large temperature anisotropy. They find that a spectral index of -2 produces the best fits with the observed data.

In a recent two-fluid model the dissipation of low-frequency Alfvén waves via a turbulent cascade was used to transport the energy from the low-frequency Alfvén waves to the ion cyclotron resonant range [35, 36]. The energy is then picked up by the plasma through resonant cyclotron interaction. Kolmogorov and Kraichnan dissipation processes were investigated. The idea of a turbulent cascade has been developed already some time before [37, 38]. The model reproduces the observed data well, including the high anisotropy of proton temperatures in the corona.

Gravitational damping of low-frequency Alfvén waves has been investigated as a possible mechanism to dissipate the wave energy into particle acceleration [39, 40]. With a two-fluid model using dissipation of Alfvén waves by gravity damping the experimental observations of the heating of the solar corona and solar wind acceleration could be reproduced reasonably well [40]. The advantage of this approach is that it is a non-resonant heating process and the necessary Alfvén waves are in the frequency range between 0.001 to 0.01 Hz. Alfvén waves of these frequencies are known to exist in the solar atmosphere, which is were the peak of the photospheric power spectrum is located. However, this approach was strongly contested by McKenzie and Axford who claimed that this gravitational damping of Alfvén waves results from not treating the problem self-consistently [41]. This disagreement could not be resolved during the workshop.

A different approach to understand the energetics of coronal heating and solar wind acceleration is by using a semi-empirical steady-state axial symmetric MHD model of the solar corona [42, 43]. The model inputs are the two-dimensional electron density and the magnetic field structure, which includes the radial dependence from Ulysses measurements, a multipolar expansion (dipole, quadrupole, and octupole), and a split monopole to define the current sheet. The heating function is then chosen such that resulting proton speed and temperature (actually the effective temperature) agree with the observations. Thus, one obtains the radial profile of the heating function for the coronal holes and the interstream region, without any assumption on the energy source and their dissipation. Once an extension to a two- or multi-fluid model has been accomplished this approach will be a valuable tool to understand the energy input in the solar corona.

2.2. Origin of slow solar wind

Slow solar wind is much more complicated to understand than the fast solar wind, since it is not constant, its properties vary on all time scales, and it has a filamentary structure. Different source locations of the slow solar wind are under discussion: the edges of the polar coronal holes, edges of streamer structures, or smaller loops structures in the equatorial region of the Sun. All

these source locations need magnetic reconnection processes to open up magnetic field lines to release plasma into space. It could well be that the slow solar wind has contributions from several sources. The understanding of the slow solar wind has not much advanced since the SOHO 7 workshop and very little material was available regarding the acceleration of slow solar wind during the meeting.

One possible source of the slow solar wind, which was discussed in the working group could be the small-scale fluctuations, the blobs or bubbles as they are called, with a mass of a blob of about 10^{11} kg. The blobs were associated with upwelling loops and are kind of tracers for the particle flux in the streamer belt are carried along in the equatorial slow wind. These blobs all have about the same speed, which approaches values typical for slow solar wind at distance of 30 solar radii. The acceleration of the slow solar wind is close to 4 m/s^2 and the profile is consistent with an isothermal expansion at $T \approx 1.1 \cdot 10^6$ K [4]. The working group concluded that the blobs could contribute about 10% to the flux of the slow solar wind.

Compared to coronal holes, less data are available about the physical parameters of possible source locations of the solar wind. The quiet-Sun densities are systematically higher than the coronal hole densities by a factor of about two to ten [2, 14]. Moreover, for the 1996 solar minimum the electron density and temperature were determined for equatorial regions from the solar limb out to 1.2 $R_\odot$ [44, 45]. On average the electron temperature in the equatorial regions is 1.2 MK close to the limb and rises to 1.4 MK at 1.2 $R_\odot$ [44], has a maximum of 1.6 MK at 1.35 $R_\odot$ and decreases further out [45]. At the solar limb the electron density is $5 \cdot 10^8$ cm^{-3}, $1.5 \cdot 10^8$ cm^{-3} at 1.1 $R_\odot$ [44], and $7 \cdot 10^4$ cm^{-3} at 4 $R_\odot$ [45]. Also David et al. [15] give an electron temperature profile for the equatorial region of the quiet corona (see Figure 5).

3. CONCLUSIONS

At lot of progress has been made, in particular in the understanding of the formation of solar wind originating from coronal holes. Instead of summarizing these accomplishments let us list what, in our opinion, is still missing in the understanding of solar wind acceleration in coronal holes.

- Detailed observations of wave spectra at a few solar radii in the frequency range up to 10^3 Hz and beyond are needed. Low-frequency (0.001–0.1 Hz) Alfvén waves dominate the power spectrum of fluctuations in the solar wind beyond 0.3 AU. Alfvén waves of higher frequency (> 10 Hz) have not been observed but there are plenty of theories for their origin (see e.g., Cranmer et al. [34]).
- The measurement of the distribution functions of particles in the inner solar corona is needed. The choice of distribution function has a big influence on the results of the theoretical models. Typically, double-Maxwellian distributions are used in current theoretical models. Unexpectedly large line widths of H^0 atoms and O^{5+} ions were observed by SOHO/UVCS, which are thought to be the result of anisotropic velocity distributions and are not consistent with purely thermal motions, e.g., Maxwellian distributions [11].
- The theory heating function needs considerable attention. Some authors use ad hoc heating functions, other authors use heating functions derived from wave dissipation under certain assumptions. However, a self-consistent heating function is still missing.
- Optical observations of alpha particles densities close to the Sun would be very interesting to compare with calculations from three-fluid models. Obviously, one cannot measure these densities directly by optical means, but perhaps there is a clever scheme involving He^+ lines or some other way. Three-fluid and multi-fluid models predict that alpha particle densities should be largely enhanced at heights around 0.5 $R_\odot$ with $n_\alpha / n_p \approx 0.5$ [13, 28, 31]. This ratio represents a 10-fold enhancement compared to the average solar wind value.

ACKNOWLEDGEMENTS

The authors gratefully acknowledge help from J.G. Doyle, J.V. Hollweg, D.J. Mullan, and K. Wilhelm. This work was supported by the Swiss National Science Foundation.

4. REFERENCES

[1] K. Wilhelm, "SUMER observations of the quiet Sun: Transition region and low corona." *Adv. Space Rec.*, (1999) in press.

[2] G.A. Doschek, J.T. Mariska, H.P. Warren, J.M. Laming, K. Wilhelm, P. Lemaire, U. Schühle, and T.G. Moran, "Electron densities in the solar polar coronal holes from density-sensitive line ratios of Si VIII and S X." *Astrophys. Jou.* **482**, (1997) L109–L112.

[3] K. Wilhelm, E. Marsch, B.N. Dwivedi, D.M. Hassler, P. Lemaire, A.H. Gabriel, and M.C.E. Huber, "The solar corona above polar coronal holes as seen by SUMER on SOHO." *Astrophys. Jou.* **500**, (1998) 1023–1038.

[4] E. Antonucci, *Solar wind acceleration region*. SOHO-8, Paris, ESA, (1999) this volume.

[5] K. Wilhelm, I.E. Dammasch, E. Marsch, and D.M. Hassler, "On the source regions of the fast solar wind in polar coronal holes." *Astron. Astrophys.*, (1999) in press.

[6] L. Ofman, M. Romoli, G. Poletto, G. Noci, and J.L. Kohl, "Ultraviolet Coronagraph Spectrometer observations of density fluctuations in the solar wind." *Astrophys. Jou.* **491**, (1997) L111–L114.

[7] L. Ofman, M. Romoli, G. Poletto, G. Noci, and J.L. Kohl, "Ultraviolet Coronagraph Spectrometer Observations of Density Fluctuations in the Solar

Wind." *Astrophys. Jou.* **507**(2), (1998) L189–L189.

[8] C.E. DeForest and J.B. Gurman, "Observation of Quasi-periodic Compressive Waves in Solar Polar Plumes." *Astrophys. Jou.* **501**, (1998) L217–L220.

[9] L. Ofman, V.M. Nakariakov, and C.E. DeForest, "Slow magnetosonic waves in coronal plumes." *Astrophys. Jou.* **514**, (1999) 441–447.

[10] J.G. Doyle, L. Teriaca, and D. Banerjee, "Coronal Hole Diagnostics out to 8 $R_{\odot}$." *Astron. Astrophys.*, (1999) in press.

[11] J.L. Kohl, G. Noci, E. Antonucci, G. Tondello, M.C.E. Huber, S.R. Cranmer, L. Strachnan, A.V. Panasyuk, L.D. Gardner, M. Romoli, S. Fineschi, D. Dobrzycka, J.C. Raymond, P. Nicolosi, O.H.W. Siegmund, D. Spadaro, C. Benna, A. Ciaravella, S. Giordano, S.R. Habbal, M. Karovska, X. Li, R. Martin, J.G. Michels, A. Modigliani, G. Naletto, R.H. O'Neal, C. Pernechele, G. Poletto, P.L. Smith, and R.M. Suleiman, "UVCS/SOHO empirical determinations of anisotropic velocity distributions in the solar corona." *Astrophys. Jou.* **501**, (1998) L127–L131.

[12] M. Guhathakurta, A. Fludra, S.E. Gibson, D. Biesecker, and R. Fisher, "Physical properties of a coronal hole from a coronal diagnostic spectrometer, Mauna Loa coronagraph, and LASCO observations during the Whole Sun Month." *J. Geophys. Res.* **104**(A5), (1999) 9801–9808.

[13] R. Esser, S. Fineschi, D. Dobrzyka, S.R. Habbal, R.J. Edgar, J.C. Raymond, J.L. Kohl, and M. Guhathakurta, "Plasma properties in coronal holes derived from measurements of minor ion spectral lines and polarized white light intensity." *Astrophys. Jou.* **510**, (1999) L63–L67.

[14] S. Koutchmy, "Study of the June 30, 1973 transpolar coronal hole." *Solar Physics* **51**, (1977) 399–407.

[15] C. David, A.H. Gabriel, F. Bely-Dubau, A. Fludra, P. Lemaire, and K. Wilhelm, "Measurement of the electron temperature gradient in a solar coronal hole." *Astron. Astrophys.* **336**, (1998) L90–L94.

[16] G. Del Zanna and B.J.I. Bromage, "The elephant's trunk: Spectroscopic diagnostic applied to SOHO/CDS observations of the August 1996 equatorial coronal hole." *J. Geophys. Res.* **104**(A5), (1999) 9753–9766.

[17] P. Wurz, M.R. Aellig, F.M. Ipavich, S. Hefti, P. Bochsler, A.B. Galvin, H. Grünwaldt, M. Hilchenbach, F. Gliem, and D. Hovestadt, "The iron, silicon, and oxygen abundance in the solar wind measured with SOHO/CELIAS/MTOF." *Phys. Chem. Earth (C)* **24**(4), (1999) 421–426.

[18] J.T. Nolte, A.S. Krieger, A.F. Timothy, R.E. Gold, E.C. Roelof, G. Vaiana, A.J. Lazarus, J.D. Sullivan, and P.S. Mcintosh, "Coronal holes as source of solar wind." *Solar Physics* **46**, (1976) 303–322.

[19] E. Marsch, K.-H. Mühlhauser, H. Rosenbauer, R. Schwenn, and F.M. Neubauer, "Solar wind helium ions: Observations of the HELIOS solar probes between 0.3 and 1 AU." *J. Geophys. Res.* **87**(A1), (1982) 35–51.

[20] P. Bochsler, "Velocity and abundance of silicon ions in the solar wind." *J. Geophys. Res.* **94**(A3), (1989) 2365–2373.

[21] J. Schmid, P. Bochsler, and J. Geiss, "Velocity of iron ions in the solar wind." *J. Geophys. Res.* **92**(A9), (1987) 9901–9906.

[22] S. Hefti, H. Grünwaldt, F.M. Ipavich, P. Bochsler, D. Hovestadt, M.R. Aellig, M. Hilchenbach, R. Kallenbach, A.B. Galvin, J. Geiss, F. Gliem, G. Gloeckler, B. Klecker, E. Marsch, E. Möbius, M. Neugebauer, and P. Wurz, "Kinetic properties of solar wind minor ions and protons measured with SOHO/CELIAS." *J. Geophys. Res.* **103**(A12), (1998) 29697–29704.

[23] R.R. Grall, W.A. Coles, M.T. Klinglesmith, A.R. Breen, P.J.S. Williams, J. Markkanen, and R. Esser, "Rapid acceleration of the polar solar wind." *Nature* **379**, (1996) 429–432.

[24] E. Marsch, C.-Y. Tu, P. Heinzel, K. Wilhelm, and W. Curdt, "Proton and hydrogen temperatures at the base of the solar polar corona." *Astron. Astrophys.* **347**, (1999) 676–683.

[25] P. Riley, S.J. Bame, B.L. Barraclough, W.C. Feldman, J.T. Gosling, G.W. Hoogeveen, D.J. McComas, J.L. Phillips, B.E. Goldstein, and M. Neugebauer, "Ulysses solar wind plasma observations at high latitudes." *Adv. Space Res.* **20**(1), (1997) 15–22.

[26] B.L. Barraclough, W.C. Feldman, J.T. Gosling, D.J. McComas, J.L. Phillips, and B.E. Goldstein, *He abundance variations in the solar wind: Observations from Ulysses*. Solar Wind Eight, Dana Point, CA, USA, Eds. D. Winterhalter, J.T. Gosling, S.R. Habbal, W.S. Kurth and M. Neugebauer, AIP Press, (1995) 277–280.

[27] J.F. McKenzie, M. Banaszkiewicz, and W.I. Axford, "Acceleration of the high speed solar wind." *Astron. Astophys.* **303**, (1995) L45–L48.

[28] A. Bürgi, "Proton and alpha particle fluxes in the solar wind: Results of a three-fluid model." *J. Geophys. Res.* **97**, (1992) 3137–3150.

[29] R. Esser and S.R. Habbal, "Coronal heating and plasma parameters at 1 AU." *Geophys. Res. Lett.* **22**(19), (1995) 2661–2664.

[30] A. Czechowski, R. Ratkiewicz, J.F. McKenzie, and W.I. Axford, "Heating and acceleration of minor ions in the solar wind." *Astron. Astrophys.* **335**, (1998) 303–308.

[31] R. Bodmer and P. Bochsler, "Fractionation of minor ions in the solar wind acceleration process." *Phys. Chem. Earth* **23**(5–6), (1998) 683–688.

[32] Y.Q. Hu, R. Esser, and S.R. Habbal, "A four-fluid turbulence-driven solar wind model for preferential acceleration and heating of heavy ions." *Astrophys. J.*, (1999) in press.

[33] C.-Y. Tu and E. Marsch, "Two-fluid model for heating of the Solar corona and acceleration of the solar wind by high-frequency alfvén waves." *Solar Physics* **171**, (1997) 363–391.

[34] S.R. Cranmer, G.B. Field, and J.L. Kohl, "Spectroscopic constraints on models of ion-cyclotron resonance heating in the polar solar corona and high speed solar wind." *Astrophys. Jou.* **518**(2), (1999) 937–947.

[35] X. Li, S.R. Habbal, J.V. Hollweg, and R. Esser, "Heating and cooling of protons by turbulence-driven ion cyclotron waves in the fast solar wind." *J. Geophys. Res.* **104**(A2), (1999) 2521–2535.

[36] J.V. Hollweg, *Resonant heating and acceleration of protons and ions in coronal holes: Two-proton closure*. SOHO-8, Paris, ESA, (1999) this volume.

[37] J.V. Hollweg and W. Johnson, "Transition region, corona, and solar wind in coronal holes: some two-fluid models." *J. Geophys. Res.* **93**, (1988) 9547–9554.

[38] P.A. Isenberg, "Investigation of a turbulence driven solar wind model." *J. Geophys. Res.* **95**, (1990) 6437–6442.

[39] I.K. Khabibrakhmanov and D.J. Mullan, "Gravitational damping of Alfvén waves in stellar atmospheres and winds." *Astrophys. J.* **430**, (1994) 814–823.

[40] I. Cuseri, D. Mullan, G. Noci, and G. Poletto, "Heating and acceleration of the solar wind via gravity damping of Alfvén waves." *Astrophys. J.* **514**, (1999) 989–1012.

[41] W.I. Axford and J.F. McKenzie, "Coronal heating and wind acceleration." *ESA* **SP-446**, (1999) submitted.

[42] E.C. Sittler and M. Guhathakurta, "Semi-empirical MHD model of the corona-interplanetary medium." *Astrophys. Jou.*, (1999) to be published.

[43] M. Guhathakurta and E.C. Sittler, "Semi-empirical MHD model of the corona-interplanetary medium during the Whole-Sun Month." *J. Geophys. Res.*, (1999) to be published.

[44] A. Fludra, G. Del Zanna, D. Alexander, and B.J.I. Bromage, "Electron density and temperature of the lower solar corona." *J. Geophys. Res.* **104**(A5), (1999) 9709–9720.

[45] S.E. Gibson, A. Fludra, F. Bagenal, D. Biesecker, and G. Del Zanna, "Solar minimum streamer densities and temperatures using Whole Sun Month coordinated data sets." *J. Geophys. Res.* **104**(A5), (1999) 9691–9699.